Springer

Journal of Mechanical Science and Technology 23 (2009) 475~488

Journal of Mechanical Science and Technology

www.springerlink.com/content/1738-494x
DOI 10.1007/s12206-008-1112-3

A series solution for spatially coupled deflection analysis of thin-walled Timoshenko curved beam with and without elastic foundation †

Nam-Il Kim and Dong Ku Shin*

Department of Civil and Environmental Engineering, Myongji University, San 38-2 Nam-Dong, Yongin, Kyonggi-Do 449-728, Korea

(Manuscript Received May 29, 2008; Revised August 20, 2008; Accepted November 15, 2008)

Abstract

The exact solutions for the spatially coupled deflection and the normal stress at an arbitrary location of a cross-section of the thin-walled Timoshenko curved beam with symmetric and non-symmetric cross-sections with and without two types of elastic foundations are newly presented using series solutions for the displacement parameters. The equilibrium equations and the force-deformation relations are derived from the elastic strain energy including the effects of shear deformation and the axial-flexural-torsional coupling, and the strain energy considering the foundation effects. The explicit expressions for displacement parameters are derived by applying the power series expansions of displacement components to the simultaneous ordinary differential equations. Next, the element stiffness matrix is determined by using the force-deformation relationships. The normal stress at any arbitrary location of the cross-section for a curved beam is evaluated from the stiffness matrix. To verify the validity and the accuracy of this study, the displacements and the normal stresses of curved beams are presented and compared with the analytical solutions, the finite element results using the isoparametric curved beam elements based on the Lagrangian interpolation polynomial, and the detailed three-dimensional analysis results using the shell elements of SAP2000.

Keywords: Thin-walled; Curved beam; Stiffness matrix; Shear deformation; Elastic foundation

1. Introduction

Thin-walled curved beam structures have been used in many civil, mechanical, and aerospace engineering applications such as curved wire, curved girder bridges, turbomachinery blades, tire dynamics, and stiffeners in aircraft structures, and the behavior of thin-walled members with open and closed cross-sections has been investigated extensively since the early works of Vlasov [1]. Also, monographs by Dabrowski [2] and Heins [3] are useful references for the thin-walled curved beam theory and its application. For the static and dynamic analyses of curved structures, the curved beam elements [4-26] based on the curvilinear strain description have generated a great deal of interest among researchers in recent years. Modeling of curved structures by means of lower-order isoparametric beam elements leads to excessively stiff behavior (called shear locking) in the thin regimes. Classical curved beam elements, when used for modeling thin and deep arches also exhibited excessive bending stiffness (called membrane locking) in approximating inextensional bending response. Up to the present, considerable research has been performed to overcome these shear and membrane locking phenomena. Reduced integration [4, 5] of shear and membrane energies is widely used for eliminating one or more higher-order components in the strain distribution which leads to spurious kinematic modes in their respective thin limits. However indiscriminate use of reduced integration can introduce zero energy modes. Prathap and Babu [6], Babu and Prathap [7]

† This paper was recommended for publication in revised form by Associate Editor Maenghyo Cho

*Corresponding author. Tel.: +82 31 330 6416, Fax.: +82 31 336 9705
E-mail address: dkshin@mju.ac.kr

proposed a field-consistency approach, which identifies the spurious constraint of the inconsistent strain field and drops them in advance. Unlike the reduced integration method, the field consistency approach ensures a variationally correct and orthogonally consistent strain field. But both these methods reduce the order of strain interpolation and suffer from lower convergence rate. Also, curved beam elements based on displacement fields derived from assumed independent strain fields exhibited no locking behavior [8-10]. Applying the assumed polynomials for the strain fields, the strain-displacement relations are solved to get general solutions for the displacement fields. Kim and Park [11] and Lee and Kim [12] proposed two-noded hybrid-mixed isotropic and unisotropic curved beam elements, respectively, with internal nodeless degrees and consistent stress parameters based on the Hellinger-Reissner variational principle without locking phenomena and stress oscillations. Wang and Chen [13] presented a locking-free meshless curved beam formulation based on the stabilized conforming nodal integration. Recently, Kim and Kim [14] presented a centroid-shear center formulation, which overcomes the drawback of previous curved beam theory based on the centroid formulation, for the spatially coupled deflection and free vibration analyses of thin-walled curved beams with non-symmetric cross-sections. Kim *et al.* [15] derived an elastic strain energy considering the shear deformation effects and then they [16] developed an isoparametric curved beam element using the reduced integration for the coupled buckling analysis. However, the result obtained from this finite curved beam element based on the classical Lagrangian interpolation polynomials is approximate and not exact. Therefore, as shown in the following numerical examples, a large numbers of curved beam elements are needed to obtain accurate results. Particularly, in evaluation of the normal stress of cross-section of curved beam by using the finite beam element, its error becomes larger because it is difficult to construct the displacement functions that satisfy the normal strain of cross-section which involves derivatives of displacements.

On the other hand, a few researchers have been interested in the development of curved beam element using the displacement fields which satisfy homogeneous forms of equilibrium equations. Kim *et al*. [17] derived the stiffness and the mass matrices, respectively, from the strain energy and the kinetic energy by using the natural shape functions of the exact in-plane displacements which are obtained from an integration of the differential equations of a thin circular beam element in static equilibrium. This element gave exact results for static problems in the case of concentrated loads because the shape functions of the element are exact in statics. Zhang and Di [18] presented new accurate two-noded finite elements which are free from shear and membrane locking and are derived from the potential energy principle and the Hellinger-Reissner functional principle, respectively. Raveendranath *et al*. [19] developed two-noded locking free curved beam elements, for which a cubic polynomial field was assumed a priori and the polynomial interpolations for the axial displacement and the twisting angle were derived employing force-moment and moment-shear equilibrium equations. Friedman and Kosmatka [20] and Litewka and Rakowski [21] developed the locking-free two-noded (three DOF per node) curved beam element based on exact displacement functions in algebraic-trigonometric form, which satisfy the element equilibrium equations. Also Litewka and Rakowski [22] derived the approximate polynomial equivalents of the functions presented in Ref. [21] by expanding the trigonometric functions into the power series. However, most of these studies are restricted to two dimensional problems and based on explicit analytical solutions of homogeneous equations.

The complicated problems for the analysis of curved beam on elastic foundation are frequently encountered due to additional parameters related to the foundation effects. There exists a wide body of literature [27-32] on the analysis of beams resting on elastic foundation since the early works of Hetenyi [27] who developed the differential equation approach. The static and dynamic cases have been studied extensively, and the subjects are covered in great depth by Volterra [28, 29]. Chakraborty and Sarkar [30] presented a stochastic finite element method for analysis of a curved beam on uncertain elastic foundation. In their study, the finite element solution has been obtained by using the Neumann expansion method within the framework of Monte Carlo simulation. Aköz and Kadioğlu [31] developed a mixed finite element formulation for circular beams on the Winkler foundation. Lee *et al*. [32] derived the governing differential equations for the out-of-plane free vibration of circular curved beams resting on Winkler-type foundations and solved numerically by using the Runge-Kutta method.

Even though a significant amount of research has been conducted on development of improved curved beam element, to the authors' knowledge, there has been no study on the evaluation of the exact solutions for the spatially coupled deflection analysis of shear deformable thin-walled curved beams with non-symmetric cross-section in the literature. Moreover, it has not been reported on the exact evaluation of the normal stress at an arbitrary location of non-symmetric cross-section of curved beam. It is well known that the elastic behavior of thin-walled curved beam with non-symmetric cross-section considering the shear deformation effects is very complex due to the coupling effect of extensional, bending, and torsional deformations, as can be seen in seven simultaneous second-order ordinary differential equations. Accordingly, many have researchers thought that it is very difficult to evaluate the exact solutions for the spatially coupled deflection and the normal stress of thin-walled curved beam with non-symmetric cross-section due to an aforementioned reason.

The purpose of this study is to present, for the first time, the exact solutions for the coupled deflection and the normal stress at an arbitrary location of cross-section of shear deformable thin-walled curved beam with and without two-types of elastic foundation. The important points are summarized as follows:

1) The equilibrium equations and the force-deformation relations of the curved beam on two-types of elastic foundations considering the shear deformation effects are newly derived.
2) The element stiffness matrix of curved beam on elastic foundation is evaluated based on the power series expansions of displacement components.
3) The evaluation procedure for the normal stress at any arbitrary location of non-symmetric cross-section of a curved beam subjected to an external force is newly presented.
4) To demonstrate the accuracy and the validity of this study, numerical solutions are presented and compared with analytical solutions and finite element solutions developed by Kim *et al*. [16] using the isoparametric curved beam elements and shell elements of SAP2000 [33].

2. Equilibrium equations and force-deformation relations

In this section, the equilibrium equations and the force-deformation relations of a curved beam considering the shear deformation effects and the non-symmetric thin-walled cross-sections are derived from the energy principle.

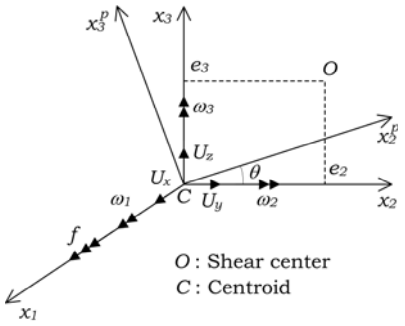

(a) Displacement parameters

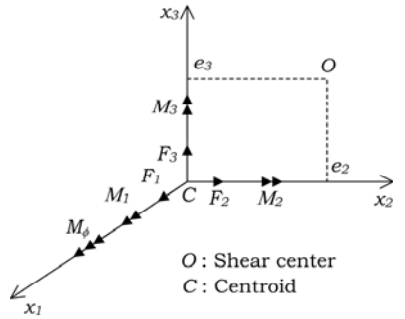

(b) Stress resultants

Fig. 1. Notation for displacement parameters and stress resultants.

Figs. 1(a) and 1(b) show the displacement parameters and the stress resultants of thin-walled curved beams, respectively. In Fig. 1(a), x_2^p and x_3^p mean principal axes defined at the centroid and θ is the angle between x_2^p and x_2 axes in the counter-clockwise direction. U_x, U_y, U_z, and ω_1, ω_2, ω_3 are the rigid body translations and the rotations of the cross-section with respect to x_1, x_2, and x_3 axes, respectively; f is the displacement parameter measuring warping deformations. Also F_1, F_2, and F_3 are the axial and shear forces acting at the centroid; M_1 is the total twist moment with respect to the centroidal axis; M_2 and M_3 are the bending moments with respect to x_2 and x_3 axes, respectively, and M_ϕ is the bimoment. The elastic strain energy of the thin-walled curved beam considering the effects of shear deformation due to the bending and the restrained warping, the non-symmetric cross-section, and the thickness-curvature is given by Ref.

[15].

$$\Pi_E = \frac{1}{2}\int_o^l \left[EA\left(U_x' + \frac{U_z}{R}\right)^2 + E\hat{I}_2\left(\omega_2' - \frac{U_x'}{R} - \frac{U_z}{R^2}\right)^2 \right.$$
$$+ E\hat{I}_3\left(\omega_3' - \frac{\omega_1}{R}\right)^2 + E\hat{I}_\phi f'^2 + 2E\hat{I}_{\phi 2}\left(\omega_2' - \frac{U_x'}{R} - \frac{U_z}{R^2}\right) f'$$
$$- 2E\hat{I}_{\phi 3}\left(\omega_3' - \frac{\omega_1}{R}\right) f' - 2E\hat{I}_{23}\left(\omega_3' - \frac{\omega_1}{R}\right)\left(\omega_2' - \frac{U_x'}{R} - \frac{U_z}{R^2}\right)$$
$$+ GJ\left(\omega_1' + \frac{\omega_3}{R}\right)^2 + GA_2\left(U_y' - \omega_3\right)^2 + GA_3\left(U_z' - \frac{U_x}{R} + \omega_2\right)^2$$
$$+ GA_r\left(\omega_1' + \frac{\omega_3}{R} + f\right)^2 + 2GA_{23}\left(U_y' - \omega_3\right)\left(U_z' - \frac{U_x}{R} + \omega_2\right)$$
$$+ 2GA_{2r}\left(U_y' - \omega_3\right)\left(\omega_1' + \frac{\omega_3}{R} + f\right)$$
$$\left. +2GA_{3r}\left(U_z' - \frac{U_x}{R} + \omega_2\right)\left(\omega_1' + \frac{\omega_3}{R} + f\right)\right] dx_1 \tag{1}$$

where

$$\hat{I}_2 = I_2 - \frac{I_{222}}{R}, \hat{I}_3 = I_3 - \frac{I_{233}}{R}, \hat{I}_{23} = I_{23} - \frac{I_{223}}{R}$$
$$\hat{I}_\phi = I_\phi - \frac{I_{\phi\phi 2}}{R}, \hat{I}_{\phi 2} = I_{\phi 2} - \frac{I_{\phi 22}}{R}, \hat{I}_{\phi 3} = I_{\phi 3} - \frac{I_{\phi 23}}{R} \tag{2}$$

In Eq. (1), the prime denotes differentiation with respect to the position x_1, and E and G are the Young's and shear moduli, respectively; A and J are the area and the torsional constant, respectively; I_2, I_3, I_{23}, and I_ϕ are the second moment of inertia about x_2 and x_3 axes, the product moment of inertia, and the warping moment of inertia, respectively; $I_{\phi 2}(=I_2 e_2)$ and $I_{\phi 3}(=-I_3 e_3)$ are the product moments of inertia due to the normalized warping; $I_{ijk}(i,j,k=\phi,2,3)$ are the third moments of inertia considering the thickness-curvature effect, which causes difference for displacements, twist angle, and the normal stress in the curved beam with large subtended angle and small radius. The detailed definitions of these sectional properties are presented in Ref. [15].

In this study, we consider the cross-section of thin-walled curved beam resting on an elastic foundation, as shown in Fig. 2, throughout its length, in which a more realistic and generalized representation of the elastic foundation can be accomplished by the way of a two-types of foundation model. In Fig. 2, k_y and k_z are the Winkler foundation moduli indicating the first type of foundation parameters for the transverse translations at the point (h_y, h_z), k_ω is the rotational parameter for rotation of the cross-section, and g_y and g_z denote the second type of foundation parameters (i.e., Vlasov, Pasternak and Filonenko-Borodich foundation modulus) at the point (h_y, h_z). The strain energy considering the foundation effects is given in Ref. [34].

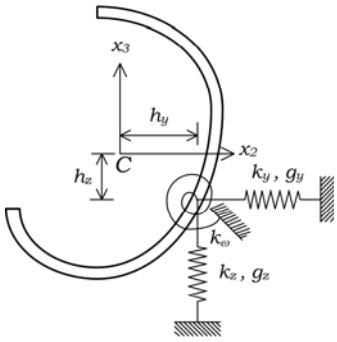

Fig. 2. Cross-section of beam on two-types of elastic foundation.

$$\Pi_F = \frac{1}{2}\int_o^l \left[k_y\left(U_y - h_z\omega_1\right)^2 + k_z\left(U_z + h_y\omega_1\right)^2 \right.$$
$$\left. + k_\omega\omega_1^2 + g_y\left(U_y' - h_z\omega_1'\right)^2 + g_z\left(U_z' + h_y\omega_1'\right)^2 \right] dx_1 \tag{3}$$

By taking the variation of Eqs. (1) and (3) with respect to seven displacement parameters, U_x, U_y, U_z, ω_1, ω_2, ω_3, and f, the coupled equilibrium equations and the force-deformation relations for the curved beam are derived and the equations are presented in the appendix.

3. Element stiffness matrix of curved beam

3.1 Exact evaluation of displacement function

The exact displacement function of the thin-walled curved beam with non-symmetric cross-section for the spatially coupled deflection analysis is evaluated. For this, we consider the displacement state vector consisting of 14 displacement parameters as follows:

$$\mathbf{d} = \langle U_x,\ U_x',\ U_y,\ U_y',\ U_z,\ U_z',\ \omega_1,\ \omega_1',\ \omega_2$$
$$\omega_2',\ \omega_3,\ \omega_3',\ f,\ f' \rangle^T \tag{4}$$

The solutions of seven displacement parameters are taken as the following infinite power series.

$$U_x = \sum_{n=0}^{\infty} a_n x^n, U_y = \sum_{n=0}^{\infty} b_n x^n,\ U_z = \sum_{n=0}^{\infty} c_n x^n$$
$$\omega_1 = \sum_{n=0}^{\infty} d_n x^n, \omega_2 = \sum_{n=0}^{\infty} e_n x^n, \omega_3 = \sum_{n=0}^{\infty} f_n x^n, f = \sum_{n=0}^{\infty} g_n x^n \quad (5)$$

By substituting Eqs. (5a-g) into the equilibrium equations of curved beam and shifting the index of power of x^n, we can get the following equation.

$$\sum_{n=0}^{\infty} \mathbf{A_n} \{a_{n+2},\ b_{n+2},\ c_{n+2},\ d_{n+2},\ e_{n+2},\ f_{n+2},\ g_{n+2}\}^T = \sum_{n=0}^{\infty} \mathbf{B_n} \{a_n, a_{n+1}, b_n, b_{n+1}, c_n, c_{n+1}, d_n, d_{n+1}, e_n, e_{n+1}, f_n, f_{n+1}, g_n, g_{n+1}\}^T \quad (6)$$

where the matrices $\mathbf{A_n}$ and $\mathbf{B_n}$ are 7×7 and 7×14 matrices, respectively, composed of coefficients. Eq. (6) can be rewritten as

$$\{a_{n+2}, b_{n+2}, c_{n+2}, d_{n+2}, e_{n+2}, f_{n+2}, g_{n+2}\}^T = \sum_{n=0}^{\infty} \mathbf{Z_n} \{a_n, a_{n+1}, b_n, b_{n+1}, c_n, c_{n+1}, d_n, d_{n+1}, e_n, e_{n+1}, f_n, f_{n+1}, g_n, g_{n+1}\}^T \quad (7)$$

where

$$\mathbf{Z_n} = \mathbf{A_n^{-1}}\, \mathbf{B_n} \quad (8)$$

The terms $a_n, b_n, \cdots, g_n$ converge to zero as $n \to \infty$. Then we put the initial integration constant vector $\mathbf{a}$ as follows:

$$\mathbf{a} = \{a_0, a_1, b_0, b_1, c_0, c_1, d_0, d_1, e_0, e_1, f_0, f_1, g_0, g_1\}^T \quad (9)$$

By substituting the integration constants obtained by Eq. (7) into Eq. (5) and rearranging Eq. (4), the displacement state vector composed of 14 displacement parameters in Eq. (4) is expressed with respect to the initial integration constant vector $\mathbf{a}$ as follows:

$$\mathbf{d} = \mathbf{X_n}\, \mathbf{a} \quad (10)$$

In each of 14 solution sets, the calculation of the coefficients by the recursive relation in Eq. (7) is continued until the contribution of the next coefficient is less than an arbitrary small number and these symbolic calculations are performed with the help of the technical computer software Mathematica [35].

The initial integration constant vector $\mathbf{a}$ can be expressed with respect to 14 nodal displacement components. The nodal displacement vector at p and q, which means the two ends of the member $(x_1 = 0,\ l)$, is defined by

$$\mathbf{U_e} = \left\langle \mathbf{U}^p, \mathbf{U}^q \right\rangle^T \quad (11)$$

where

$$\mathbf{U}^p = \left\langle U_x(0), U_y(0), U_z(0), \omega_1(0), \omega_2(0), \omega_3(0), f(0) \right\rangle^T$$
$$\mathbf{U}^q = \left\langle U_x(l), U_y(l), U_z(l), \omega_1(l), \omega_2(l), \omega_3(l), f(l) \right\rangle^T \quad (12)$$

Substituting coordinates of the ends of member $(x_1 = 0,\ l)$ into Eq. (10) and accounting for Eq. (11), the nodal displacement vector $\mathbf{U_e}$ can be obtained as follows:

$$\mathbf{U_e} = \mathbf{H}\, \mathbf{a} \quad (13)$$

Elimination of $\mathbf{a}$ from Eq. (10) using Eq. (13) yields the displacement state vector consisting of 14 displacement components.

$$\mathbf{d} = \mathbf{X_n}\, \mathbf{H}^{-1}\, \mathbf{U_e} \quad (14)$$

It should be noted that $\mathbf{X_n}\, \mathbf{H}^{-1}$ in Eq. (14) denotes the 14×14 exact interpolation matrix since the displacement state vector satisfies the homogenous form of the seven coupled equilibrium equations.

3.2 Calculation of stiffness matrix

We consider the force-deformation relations of curved beam which can be expressed in a matrix form as follows:

$$\mathbf{f} = \mathbf{S}\, \mathbf{d} \quad (15)$$

Substitution of the displacement function in Eq. (14) into Eq. (15) leads to

$$\mathbf{f} = \mathbf{S}\, \mathbf{X_n}\, \mathbf{H}^{-1}\, \mathbf{U_e} \quad (16)$$

The nodal forces at two ends of the element are evaluated as

$$\mathbf{F}^p = -\mathbf{f}(0) = -\mathbf{S}\,\mathbf{X}_\mathbf{n}(0)\,\mathbf{H}^{-1}\mathbf{U}_\mathbf{e}$$
$$\mathbf{F}^q = \mathbf{f}(l) = \mathbf{S}\,\mathbf{X}_\mathbf{n}(l)\,\mathbf{H}^{-1}\mathbf{U}_\mathbf{e} \tag{17}$$

Consequently, the element stiffness matrix of a thin-walled Timoshenko curve beam considering the non-symmetric cross-section and the foundation effect is evaluated as

$$\mathbf{F}_\mathbf{e} = \mathbf{K}\,\mathbf{U}_\mathbf{e} \tag{18}$$

where

$$\mathbf{K} = \begin{bmatrix} -\mathbf{S}\,\mathbf{X}_\mathbf{n}(0)\,\mathbf{H}^{-1} \\ \mathbf{S}\,\mathbf{X}_\mathbf{n}(l)\,\mathbf{H}^{-1} \end{bmatrix} \tag{19}$$

It is noticeable that the stiffness matrix in Eq. (19) is formed by the shape functions which are exact solutions of the equilibrium equations. Therefore, the accurate curved beam element based on the stiffness matrix developed by this study eliminates discretization errors and is free from the shear and membrane locking.

4. Exact evaluation of normal stress at an arbitrary location of cross-section

As explained previously, for evaluation of the normal stress at an arbitrary span and location of the cross-section of curved beam, the presence of coupling in the differential equations makes a closed form solution very difficult to obtain. Even in using the finite curved beam element based on the approximate interpolation polynomials, it is difficult to construct the displacement functions that satisfy the normal strain of cross-section which involves derivatives of displacements.

Referring to the study of Kim et al. [15], the normal strain-displacement relation at an arbitrary point of cross-section of curved beam is given as:

$$e_{11} = \left(U_{1,1} + \frac{U_3}{R}\right)\frac{R}{R+x_3} = \left[\left(U_x' + \frac{U_z}{R}\right) - x_2\left(\omega_3' - \frac{\omega_1}{R}\right) + x_3\omega_2' + \phi f'\right]\frac{R}{R+x_3} \tag{20}$$

To evaluate values of the displacements and the stress at an arbitrary point of cross-section of beam, we consider the member force $\mathbf{F}(x_1)$ at two ends of beam having the span length x_1 from Eq. (18) as follows:

$$\mathbf{F}(x_1) = \mathbf{K}(x_1)\,\mathbf{d}^*(l) \tag{21}$$

where $\mathbf{d}^*(l)$ denotes the displacements at two ends of beam which has the span length l and

$$\mathbf{K}(x_1) = \begin{bmatrix} -\mathbf{S}\,\mathbf{X}_\mathbf{n}(0)\,\mathbf{H}^{-1} \\ \mathbf{S}\,\mathbf{X}_\mathbf{n}(x_1)\,\mathbf{H}^{-1} \end{bmatrix} \tag{22}$$

The displacement at span x_1 of beam is evaluated as follows:

$$\mathbf{d}^*(x_1) = \tilde{\mathbf{K}}^{-1}(x_1)\mathbf{F}(x_1) \tag{23}$$

where

$$\tilde{\mathbf{K}}(x_1) = \begin{bmatrix} -\mathbf{S}\,\mathbf{X}_\mathbf{n}(0)\,\mathbf{H}^{*-1} \\ \mathbf{S}\,\mathbf{X}_\mathbf{n}(x_1)\,\mathbf{H}^{*-1} \end{bmatrix} \tag{24}$$

In Eq. (24), $\mathbf{H}^*$ is evaluated by substituting coordinates of the ends of member with its span length x_1 into Eq. (10). Therefore the displacement state vector $\mathbf{d}(x_1)$ in Eq. (4) which is composed of 14 displacement parameters at span x_1 can be expressed from Eq. (14).

$$\mathbf{d}(x_1) = \mathbf{X}_\mathbf{n}(x_1)\,\mathbf{H}^{*-1}\mathbf{d}^*(x_1) \tag{25}$$

Finally, by substituting the displacement parameters obtained from Eq. (25) into Eq. (20) and applying Hooke's law, the exact normal stress at point (x_2, x_3) of cross-section at an arbitrary span x_1 for the Timoshenko curved beam subjected to the external forces can be evaluated.

5. Isoparametric curved beam element

For comparison, the finite curved beam element based on the isoparametric beam formulation having the thin-walled cross-section and the shear deformations which has been developed by Kim *et al.* [16] is used. In this study, the 2-noded isoparametric curved beam element with 7 DOF per node is introduced to interpolate displacement parameters that are defined at the centroid. The coordinate and all displacement

parameters of the beam element can be interpolated with respect to the nodal coordinates and displacements, respectively.

The element displacement vector $\mathbf{U}_{fe}$ and force vector $\mathbf{F}_{fe}$ for the isoparametric curved beam element are defined as

$$\mathbf{U}_{fe} = \left\langle U^1,\ U^2 \right\rangle$$
$$\mathbf{U}^\eta = \left\langle U_x^\eta, U_y^\eta, U_z^\eta, \omega_1^\eta, \omega_2^\eta, \omega_3^\eta, f^\eta \right\rangle^T, \eta = 1, 2$$
$$\mathbf{F}_{fe} = \left\langle F^1,\ F^2 \right\rangle$$
$$\mathbf{F}^\eta = \left\langle F_1^\eta, F_2^\eta, F_3^\eta, M_1^\eta, M_2^\eta, M_3^\eta, M_\phi^\eta \right\rangle^T \quad (26)$$

where $\mathbf{U}^\eta$ and $\mathbf{F}^\eta$ are the nodal point displacement and force vectors, respectively.

Substituting the shape functions and cross-sectional properties into Eqs. (1) and (3) and integrating along the element length, the potential energy of the thin-walled finite curved beam element is obtained in a matrix form as

$$\prod_T = \frac{1}{2}\mathbf{U}_{fe}^{\mathrm{T}}\mathbf{K}_{fe}\mathbf{U}_{fe} - \mathbf{U}_{fe}^{\mathrm{T}}\mathbf{F}_{fe} \quad (27)$$

where $\mathbf{K}_{fe}$ is the element elastic stiffness in local coordinate. The elastic stiffness matrix is evaluated by using a reduced Gauss numerical integration scheme, and the assembly of the element stiffness matrix for the entire structure based on the coordinate transformation leads to the equilibrium matrix equation in a global coordinate system.

6. Numerical examples

To illustrate the accuracy and the practical usefulness of this study, numerical solutions for the spatially coupled deflection analysis of the thin-walled Timoshenko curved beam with symmetric and non-symmetric cross-sections are presented and compared with the analytical solutions, and the finite element results using the isoparametric curved beam elements and the shell elements of SAP2000.

6.1 Curved beam with symmetric cross-section

Fig. 3. shows the cantilevered I-beam subjected to a vertical force 100 N at the free end and its material and sectional properties. The length of the curved beam is 100 cm.

Table 1. Horizontal, vertical displacements and rotational angle at free end of the curved I-beam subjected to a vertical tip force (cm, rad.×10^{-2}).

		U_x	U_z	ω_y
Taucher [36]		-1.5331	2.4253	-4.7587
1800 shell elements		-1.543	2.421	-4.994
Isoparametric curved beam [16]	2	-1.3227	1.9839	-4.4069
	4	-1.4793	2.2976	-4.6648
	10	-1.5288	2.3971	-4.7434
	30	-1.5374	2.4145	-4.7570
	50	-1.5381	2.4159	-4.7581
This study		-1.5385	2.4167	-4.7587

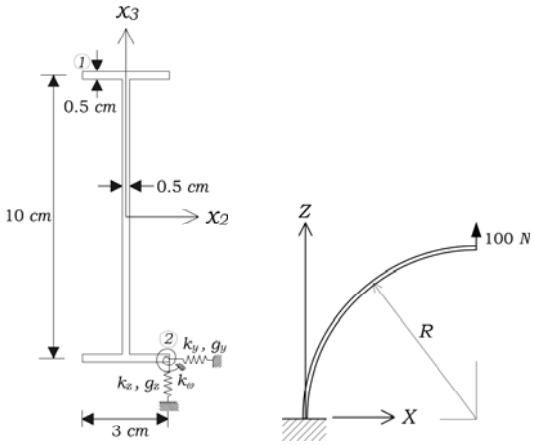

(a) Geometry of a curved beam

(b) Doubly symmetric cross-section

$A = 8$ cm^2, $E = 73000$ N/cm^2, $G = 28000$ N/cm^2,
$J = 0.66667$ cm^4, $I_2 = 116.66667$ cm^4,
$I_3 = 2.25$ cm^4, $I_\phi = 56.25$ cm^6, $I_{\phi 23} = -56.25$ cm^6,
$A_2 = 2.5$ cm^2, $A_3 = 4.77932$ cm^2, $A_r = 62.5$ cm^4,
$l = 100$ cm, $k_y = 10$ N/cm^2, $k_z = 10$ N/cm^2,
$k_\omega = 10$ N, $g_y = 10$ N, $g_z = 10$ N

(c) Material and sectional properties

Fig. 3. Cantilevered curved beam with a doubly symmetric cross-section.

First, for the curved beam without elastic foundation, the horizontal and vertical displacements, and rotational angle at the centroid of free end of beam obtained from the stiffness matrix method developed by this study are evaluated and presented in Table 1. For comparison, the results by finite element solutions using the various numbers of isoparametric curved beam elements and the SAP2000 analysis are also presented in Table 1. The SAP2000 results are obtained by using a total of 1800 4-noded shell ele-

ments. Also given in Table 1 is the analytical solution obtained from Castigliano's energy theorem [36] considering shear deformation effect. The responses at the free end of a cantilevered curved beam using the energy theorem subjected to a vertical force are given as

$$U_x = -\frac{PR^3}{2EI_2} + \frac{PR}{2EA} - \frac{PR}{2GA_3}$$
$$U_z = \frac{\pi PR^3}{4EI_2} + \frac{\pi PR}{4EA} + \frac{\pi PR}{4GA_3}$$
$$\omega_2 = -\frac{PR^2}{EI_2} \tag{28}$$

It can be found from Table 1 that the results by this study using only a single element are found to be in excellent agreement with the finite element results using 50 curved beam elements and analytical solutions. And the present results are in good agreement with those of SAP2000 analysis. It should be noted that the displacements and rotational angle obtained from a single element based on the present study are exact since these satisfy the homogenous form of the equilibrium equations.

Next, the normal stresses at points ① and ② of the mid-span of beam (Fig. 3(b)) are evaluated and compared with the results by SAP2000 analysis in Table 2. The correlation between the two sets of results is seen to be excellent for the points considered.

Table 2. Normal stresses at the mid-span of the curved I-beam subjected to a vertical tip force (N/cm^2).

Points	This study	shell elements
①	-178.88	-177.09
②	209.37	207.20

Table 3. Displacements, twisting and rotational angles at free end of the curved I-beam on elastic foundation subjected to a vertical tip force (cm, rad.×10^{-2}).

	Isoparametric curved beam [16]			This study
	4	20	50	
U_x	-0.27901	-0.26703	-0.26659	-0.26650
U_y	0.37605	0.38767	0.38798	0.38804
U_z	0.54360	0.55317	0.55346	0.55352
ω_1	-10.560	-10.874	-10.882	-10.883
ω_2	-1.3330	-1.3418	-1.3420	-1.3420
ω_3	-1.9528	-2.0186	-2.0200	-2.0202

We consider the curved beam supported partially on two-types of elastic foundation as shown in Fig. (3b). It is assumed that the foundation terminates at the beam ends and the foundation parameters are $k_y = k_z$ = 10 N/cm^2 and $k_\omega = g_y = g_z$ = 10 N. The behavior of a beam on an elastic foundation, which is partially supported, is very complex due to the coupling effects of extensional, flexural, and torsional deformations.

Table 3 shows the comparison between the solutions by this study and those by various numbers of isoparametric curved beam elements for the coupled displacements, twisting and rotational angles at the centroid of the free end. From Table 3, it is seen that as many as 50 isoparametric curved beam elements are needed to obtain accurate results when compared with the present results. In Fig. 4, the convergence behavior of isoparametric beam elements for the normalized displacements, twisting, and rotational angles with respect to the values from the present exact solutions is displayed. As can be seen in Fig. 4, the convergence for the normalized displacement U_y and rotational angle ω_2 are much faster than those for ω_1 and ω_3. Another convergence study has been conducted for the coupled displacements, twisting and rotational angles of the beam with the increase of the number of terms in power series expansion and the deformations with various numbers of terms are presented in Table 4. It is observed that the coupled values gradually approach the exact solutions as the number n increases.

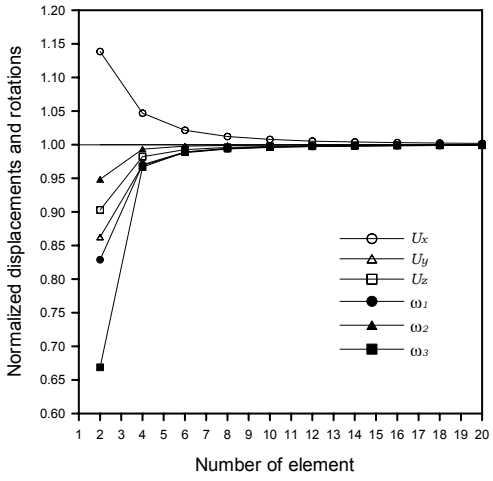

Fig. 4. Convergence behavior of the isoparametric curved beam elements for the normalized displacements and rotations at free end of the curved I-beam on elastic foundation

Table 4. Convergence of the displacements, twisting and rotational angles of the curved I-beam on elastic foundation with the increase of n (cm, rad.×10^{-2}).

	Number of terms in series expansion, n			
	10	20	30	40
U_x	-0.37197	-0.18494	-0.26636	-0.26650
U_y	0.95080	0.57368	0.38830	0.38804
U_z	0.86186	0.42522	0.55329	0.55352
ω_1	1.6311	1.9728	-10.861	-10.883
ω_2	-2.2253	-1.0950	-1.3416	-1.3420
ω_3	4.3928	3.0574	-2.0117	-2.0202

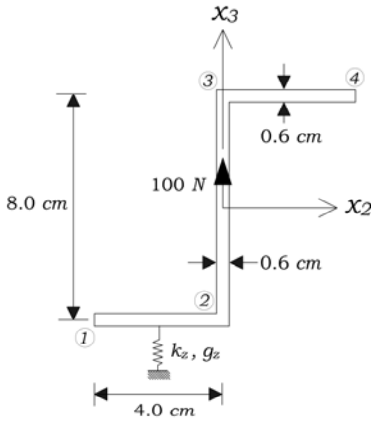

(a) Non-symmetric open section

$A = 9.6$ cm^2, $E = 73000$ N/cm^2, $G = 28000$ N/cm^2, $J = 1.152$ cm^4, $I_2 = 102.4$ cm^4, $I_3 = 25.6$ cm^4, $I_{23} = 38.4$ cm^4, $I_\phi = 256.0$ cm^6, $I_{\phi 22} = -204.8$ cm^6, $I_{\phi 23} = -256.0$ cm^6, $A_2 = 3.79228$ cm^2, $A_3 = 4.43143$ cm^2, $A_{23} = 0.31958$ cm^2, $A_r = 47.05882$ cm^4, $l = 100$ cm

(b) Material and sectional properties

Fig. 5. Non-symmetric cross-section of the cantilevered beam subjected to a vertical tip force.

6.2 Curved beam with non-symmetric open section

The purpose of this example is to evaluate the spatially coupled displacements, twisting and rotational angles, and normal stress at arbitrary span and point of cross-section for non-symmetric curved beam subjected to an external force. Fig. 5 shows the dimension of the non-symmetric cross-section of cantilevered curved beam subjected to a vertical tip force at the free end. For a curved beam neglecting the foundation effects, Table 5 gives the comparison of results using a single element by this study with those using various numbers of isoparametric beam elements and

Table 5. Displacements, twisting and rotational angles at free end of the curved beam with non-symmetric cross-section subjected to a vertical tip force (cm, rad.×10^{-2}).

	Isoparametric curved beam [16]		shell elements	This study
	20	50		
U_x	-3.9645	-3.9698	-3.928	-3.9708
U_y	-9.1336	-9.1500	-9.172	-9.1531
U_z	6.2246	6.2353	6.168	6.2374
ω_1	15.422	15.448	14.88	15.453
ω_2	-12.384	-12.392	-12.47	-12.394
ω_3	-8.7558	-8.7556	-9.013	-8.7555

Table 6. Normal stresses at the mid-span of the curved beam with non-symmetric cross-section subjected to a vertical tip force (N/cm^2).

Points	This study	shell elements
①	-216.36	-219.06
②	429.51	429.43
③	-377.67	-376.14
④	187.59	183.15

1440 shell elements of SAP2000.

It can be seen from Table 5 that the present results are in excellent agreement with the solutions obtained by using 50 isoparametric beam elements and in good agreement with those from the SAP2000 analysis for all coupled displacement parameters. In Table 6, another comparison is made for the normal stresses at four different locations of the cross-section at the beam mid-span. It is seen that the present results show excellent correlations with those of SAP2000 analysis with a maximum difference within 2.37% at point ④.

To show the practical application point of view for the curved beam on an elastic foundation, the beam including the foundation effects as shown in Fig. 5 is considered. In evaluation of the foundation parameters, the analytical method studied by Vallabhan and Das [37] based on the modified 2-D Vlasov model is applied. This method uses experimentally determined values for the soil modulus of elasticity E_s and the Poisson ratio ν. If the soil is loose sand with E_s = 1750 N/cm^2 and $\nu = 0.28$, the application of the Vallabhan-Das method produces the coefficient of subgrade reaction K_s = 0.99461 N/cm^3 and g_z = 14918.52 kN. For a beam width b_B = 4 cm, the Winkler foundation modulus is $k_z = K_s b_B$ = 3.978 N/cm^2. In Table 7, the coupled displacement parame ters at the centroid of the free end by this study are

Table 7. Displacements, twisting and rotational angles at free end of the curved beam with non-symmetric cross-section on elastic foundation subjected to a vertical tip force (cm, rad.).

	Isoparametric curved beam [16]			This study
	4	20	50	
U_x	-0.35134	-0.35707	-0.35727	-0.35731
U_y	3.6671	3.3520	3.3404	3.3381
U_z	0.54427	0.56046	0.56104	0.56116
ω_1	0.27182	0.27991	0.28020	0.28026
ω_2	-0.01117	-0.01119	-0.01119	-0.01119
ω_3	0.15147	0.15416	0.15426	0.15428

compared with results from various numbers of isoparametric beam elements. Excellent agreement is observed between the results from this study using a single element and the finite element results using as many as 50 isoparametric beam elements.

6.3 Curved beam with non-symmetric closed section

In our final example, a curved girder with non-symmetric closed section and with subtended angle 90° as shown in Fig. 6 is considered. The girder is simply supported at two ends and is subjected to an eccentric lateral force 89 N at the exterior web of mid-span. In the experimental study by Fam and Turkstra [38] based on linear elastic region, plexiglass was chosen as the model material in preference to aluminum or steel. Due to its low modulus of elasticity, a reasonably sized model could be tested with very small loads to obtain a significant measurable response. Because the material properties of plexiglass are time dependent, a series of preliminary tension and bending tests were performed on specimens cut from the same sheet as the model sections. As a result of the test, the material properties are taken as $E = 275.97$ kN/cm^2 and $\nu = 0.36$. Also, the effect of loading history on the viscoelastic behavior of the plexiglass was found to be negligible if a time interval of at least 24 hours was left between loading cycles to allow the model to recover its original unstrained state.

In our final example, a curved girder with non-symmetric closed section and with subtended angle 90° as shown in Fig. 6 is considered. The girder is simply supported at two ends and is subjected to an eccentric lateral force 89 N at the exterior web of mid-span. In the experimental study by Fam and Turkstra [38] based on linear elastic region, plexiglass was chosen as the model material in preference to aluminum or steel. Due to its low modulus of elastic-

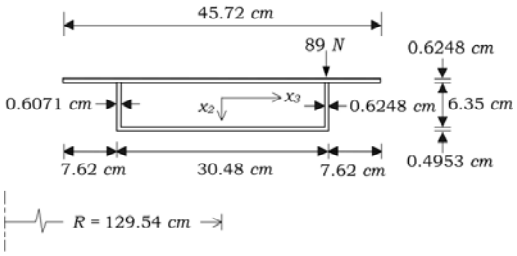

(a) Non-symmetric box section

$A = 51.870$ cm^2, $J = 1306.249$ cm^4,
$I_2 = 7973.244$ cm^4, $I_3 = 507.779$ cm^4,
$I_{23} = 1.353$ cm^4, $I_{222} = -427.197$ cm^5,
$I_{223} = -6078.562$ cm^5, $I_{233} = -9.500$ cm^5,
$I_\phi = 24539.193$ cm^6, $I_{\phi 2} = 6811.308$ cm^5,
$I_{\phi 3} = -22.924$ cm^5, $I_{\phi 22} = -225.146$ cm^6,
$I_{\phi 23} = -35838.256$ cm^6, $I_{\phi\phi 2} = 2279.427$ cm^7,
$A_2 = 4.183$ cm^2, $A_3 = 37.528$ cm^2,
$A_{23} = 0.006035$ cm^2, $A_r = 3016.378$ cm^4,
$A_{2r} = -95.755$ cm^3, $A_{3r} = 95.247$ cm^3

(b) Material and sectional properties

Fig. 6. Simply supported curved girder with non-symmetric box section.

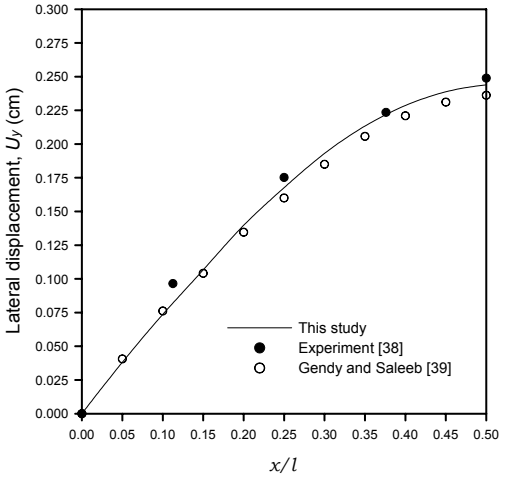

Fig. 7. Lateral displacement along the internal web of a curved box girder.

ity, a reasonably sized model could be tested with very small loads to obtain significant measurable response. Because the material properties of plexiglass are time dependent, a series of preliminary tension and bending tests were performed on specimens cut from the same sheet as the model sections. As a result of test, the material properties are taken as $E =$

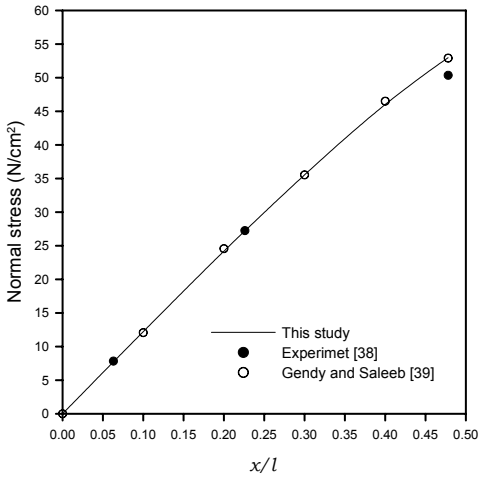

Fig. 8. Normal stress along the mid-point of the lower flange for a curved box girder.

275.97 kN/cm^2 and ν = 0.36. Also, the effect of loading history on the viscoelastic behavior of the plexiglass was found to be negligible if a time interval of at least 24 hours was left between loading cycles to allow the model to recover its original unstrained state.

The out-of-plane lateral displacement of the top flange at the location of the interior web and the normal stress at the mid-point of the bottom flange by the present study are depicted in Figs. 7 and 8, respectively. For comparison, the experimental results [38] and the solutions from 10 HMC2 curved beam elements considering shear effects developed by Gendy and Saleeb [39] are presented together. From Figs. 7 and 8, it can be found that present results are in a good agreement with the comparisons reported.

7. Conclusions

This study is the first attempt to evaluate exactly the spatially coupled deflection and the normal stress of shear deformable thin-walled curved beam with non-symmetric cross-section considering or neglecting the foundation effects. It overcomes the drawbacks arising from the use of the finite beam element based on approximate shape functions. The proposed curved beam based on the exact stiffness matrix developed by this study is not approximate but exact since the displacement functions satisfy the homogeneous form of the equilibrium equations. It should be noted that the present method requires no explicit derivation of the closed-form solutions for displacement parameters of curved beam.

Through the numerical examples, the displacements, twisting and rotational angles of the coupled curved beam by this study are shown to be in excellent agreement with the analytical solutions and the finite element solutions using the isoparametric curved beam elements and the shell elements. Particularly, this curved beam element gives an accurate normal stress at any arbitrary location of cross-section along the length with the use of only one element. It is believed that the present procedure is general enough to provide a systematic tool for exact solutions of simultaneous ordinary differential equations of the higher order.

References

[1] V. Z. Vlasov, *Thin-walled elastic beams*, 2nd Ed, National Science Foundation, Washington, DC, (1961).

[2] R. Dabrowski, *Curved thin-walled girders*, Cement and concrete association, (1968).

[3] C. P. Heins, *Bending and torsional design in structural members*, D.C. Health and Company, (1975).

[4] G. Prathap, The curved beam/deep arch/finite ring element revisited, *International Journal for Numerical Methods in Engineering*, 21 (1985) 389-407.

[5] G. Prathap and G. Bhashyam, Reduced integration and the shear-flexible beam element, *International Journal for Numerical Methods in Engineering*, 18 (1982) 195-210.

[6] G. Prathap and C. R. Babu, An isoparametric quadratic thick curved beam element, *International Journal for Numerical Methods in Engineering*, 23 (1986) 1583-1600.

[7] C. R. Babu and G. Prathap, A linear thick curved beam element, *International Journal for Numerical Methods in Engineering*, 23 (1986)1313-1328.

[8] J. K. Choi and J. K. Lim, General curved beam elements based on the assumed strain fields, *Computers and Structures*, 55 (1995) 379-386.

[9] J. K. Choi and J. K. Lim, Simple curved shear beam elements, *Communications in Numerical Methods in Engineering*, 9 (1993) 659-669.

[10] P. G. Lee and H. C. Sin, Locking-free curved beam element based on curvature, *International Journal for Numerical Methods in Engineering*, 37 (1994) 989-1007.

[11] J. G. Kim and Y. K. Park, Hybrid-mixed curved

beam elements with increased degrees of freedom for static and vibration analyses, *International Journal for Numerical Methods in Engineering*, 68 (2006) 690-706.

[12] H. C. Lee and J. G. Kim, A new hybrid-mixed composite laminated curved beam element, *Journal of Mechanical Science and Technology*, 19 (2005) 811-819.

[13] D. Wang and J. S. Chen, A locking-free meshless curved beam formulation with the stabilized conforming nodal integration, *Computational Mechanics*, 39 (2006) 83-90.

[14] N. I. Kim and M. Y. Kim, Thin-walled curved beam theory based on centroid-shear center formulation, *Journal of Mechanical Science and Technology*, 19 (2005) 597-612.

[15] K. Y. Kim, S. B. Kim and N. I. Kim, Spatial stability of shear deformable curved beams with non-symmetric thin-walled sections. I: improved stability formulation, *Computers and Structures*, 83 (2005) 2525-2541.

[16] K. Y. Kim, N. I. Kim and S. B. Kim, Spatial stability of shear deformable curved beams with non-symmetric thin-walled sections. II: F.E. solutions and parametric study, *Computers and Structures*, 83 (2005) 2542-2558.

[17] C. B. Kim. J. W. Park, S. Kim and C. Cho, A finite thin circular beam element for in-plane vibration analysis of curved beams, *Journal of Mechanical Science and Technology*, 19 (2005) 2187-2196.

[18] C. Zhang and S. Di, New accurate two-noded shear-flexible curved beam elements, *Computational Mechanics*, 30 (2003) 81-87.

[19] P. Raveendranath, G. Singh and B. Pradhan, A two-noded locking-free shear flexible curved beam element, *International Journal for Numerical Methods in Engineering*, 44 (1999) 265-280.

[20] Z. Friedman and J. B. Kosmatka, An accurate two-node finite element for shear deformable curved beams, *International Journal for Numerical Methods in Engineering*, 41 (1998) 473-498.

[21] P. Litewka and J. Rakowski, The exact thick arch finite element, *Computers and Structures*, 68 (1998) 369-379.

[22] P. Litewka and J. Rakowski, An efficient curved beam finite element, *International Journal for Numerical Methods in Engineering*, 40 (1997) 2629-2652.

[23] K. Kang, Vibration analysis of thin-walled curved beams using DQM, *Journal of Mechanical Science and Technology*, 21 (2007) 1207-1217.

[24] K. Kang and J. W. Han, Analysis of a curved beam using classical and shear deformable beam theories, *KSME International Journal*, 12 (1998) 244-256.

[25] J. Lee, Free vibration analysis of circularly curved multi-span Timoshenko beams by the pseudospectral method, *Journal of Mechanical Science and Technology*, 21 (2007) 2066-2072.

[26] J. G. Kim and Y. Y. Kim, A new higher-order hybrid-mixed curved beam element, *International Journal for Numerical Methods in Engineering*, 44 (1998) 925-940.

[27] M. Hetenyi, *Beams on elastic foundations*, Scientific Series, Vol. XVI. Ann Arbor, University of Michigan Press, (1946).

[28] E. Volterra, Bending of circular beam resting on an elastic foundation, *Journal of Applied Mechanics*, 19 (1952) 1-4.

[29] E. Volterra, Deflection of circular beams resting on elastic foundation obtained by the method of harmonic analysis, *Journal of Applied Mechanics*, 20 (1953) 227-237.

[30] S. Chakraborty and S. K. Sarkar, Analysis of a curved beam on uncertain elastic foundation, *Finite Elements in Analysis and Design*, 36 (2000) 73-82.

[31] A. Y. Aköz and F. Kadioğlu, The mixed finite element solution of circular beam on elastic foundation, *Computers and Structures*, 60 (1996) 643-651.

[32] B. K. Lee, S. J. Oh and K. K. Park, Free vibrations of shear deformable circular curved beams resting on elastic foundations, *International Journal of Structural Stability and Dynamics*, 2 (2002) 77-97.

[33] SAP 2000 NonLinear Version 6.11, *Integrated finite element analysis and design of structures*, Computers and Structures Inc., Berkeley, California, (1995).

[34] N. I. Kim, S. S. Jeon and M. Y. Kim, An improved numerical method evaluating exact static element stiffness matrices of thin-walled beam-columns on elastic foundations, *Computers and Structures*, 83 (2005) 2003-2022.

[35] S. Wolfram, *Mathematica, a system for doing mathematics by computer*, Addison-Wesley, Redwood City, California, (1988).

[36] T. R. Tauchert TR, *Energy principles in structural mechanics*, McGraw-Hill Kogakusha, LTD, (1974).

[37] C. V. G. Vallabhan and Y. C. Das, Modified Vlasov model for beams on elastic foundation, *Journal of Geotechnical Engineering*, 117 (1991) 956-966.

[38] A. R. M. Fam and C. Turkstra, Model study of horizontally curved box girder, *Journal of the Structural Division ASCE*, 102 (1976) 1097-1108.

[39] A. S. Gendy and A. F. Saleeb, On the finite element analysis of the spatial response of curved beams with arbitrary thin-walled sections, *Computers and Structures*, 44 (1992) 639-652.

Appendix

Equilibrium equations and the force-deformation relations for the curved beam

i) Equilibrium equations of curved beam

$$\begin{aligned}
&-EA\left(U_x''+\frac{1}{R}U_z'\right)+\frac{1}{R}E\hat{I}_2\left(\omega_2''-\frac{1}{R}U_x''-\frac{1}{R^2}U_z'\right)\\
&+\frac{1}{R}E\hat{I}_{\phi 2}f''-\frac{1}{R}E\hat{I}_{23}\left(\omega_3''-\frac{1}{R}\omega_1'\right)\\
&-\frac{1}{R}GA_3\left(U_z'+\omega_2-\frac{1}{R}U_x\right)-\frac{1}{R}GA_{23}\left(U_y'-\omega_3\right)\\
&-\frac{1}{R}GA_{3r}\left(\omega_1'+f+\frac{1}{R}\omega_3\right)=0
\end{aligned}\tag{A.1a}$$

$$\begin{aligned}
&GA_2\left(U_y''-\omega_3'\right)+GA_{23}\left(U_z''+\omega_2'-\frac{1}{R}U_x'\right)\\
&+GA_{2r}\left(\omega_1''+f'+\frac{1}{R}\omega_3'\right)-k_y\left(U_y-h_z\omega_1\right)\\
&+g_y\left(U_y''-h_z\omega_1''\right)=0
\end{aligned}\tag{A.1b}$$

$$\begin{aligned}
&\frac{1}{R}EA\left(U_x'+\frac{1}{R}U_z\right)-\frac{1}{R^2}E\hat{I}_2\left(\omega_2'-\frac{1}{R}U_x'-\frac{1}{R^2}U_z\right)\\
&-\frac{1}{R^2}E\hat{I}_{\phi 2}f'+\frac{1}{R^2}E\hat{I}_{23}\left(\omega_3'-\frac{1}{R}\omega_1\right)\\
&-GA_3\left(U_z''+\omega_2'-\frac{1}{R}U_x'\right)-GA_{23}\left(U_y''-\omega_3'\right)\\
&-GA_{3r}\left(\omega_1''+f'+\frac{1}{R}\omega_3'\right)+k_z\left(U_z+h_y\omega_1\right)\\
&-g_z\left(U_z''+h_y\omega_1''\right)=0
\end{aligned}\tag{A.1c}$$

$$\begin{aligned}
&-\frac{1}{R}E\hat{I}_3\left(\omega_3'-\frac{1}{R}\omega_1\right)+\frac{1}{R}E\hat{I}_{\phi 3}f'\\
&+\frac{1}{R}E\hat{I}_{23}\left(\omega_2'-\frac{1}{R}U_x'-\frac{1}{R^2}U_z\right)-GJ\left(\omega_1''+\frac{1}{R}\omega_3'\right)\\
&-GA_r\left(\omega_1''+f'+\frac{1}{R}\omega_3'\right)-GA_{2r}\left(U_y''-\omega_3'\right)\\
&-GA_{3r}\left(U_z''+\omega_2'-\frac{1}{R}U_x'\right)-k_yh_zU_y+k_zh_yU_z\\
&+\left(k_yh_z^2+k_zh_y^2+k_\omega\right)\omega_1+g_yh_zU_y''-g_zh_yU_z''\\
&-\left(g_yh_z^2+g_zh_y^2\right)\omega_1''=0
\end{aligned}\tag{A.1d}$$

$$\begin{aligned}
&-E\hat{I}_2\left(\omega_2''-\frac{1}{R}U_x''-\frac{1}{R^2}U_z'\right)-E\hat{I}_{\phi 2}f''\\
&+E\hat{I}_{23}\left(\omega_3''-\frac{1}{R}\omega_1'\right)+GA_3\left(U_z'+\omega_2-\frac{1}{R}U_x\right)\\
&+GA_{23}\left(U_y'-\omega_3\right)+GA_{3r}\left(\omega_1'+f+\frac{1}{R}\omega_3\right)=0
\end{aligned}\tag{A.1e}$$

$$\begin{aligned}
&-E\hat{I}_3\left(\omega_3''-\frac{1}{R}\omega_1'\right)+E\hat{I}_{\phi 3}f''\\
&+E\hat{I}_{23}\left(\omega_2''-\frac{1}{R}U_x''-\frac{1}{R^2}U_z'\right)+\frac{1}{R}GJ\left(\omega_1'+\frac{1}{R}\omega_3\right)\\
&-GA_2\left(U_y'-\omega_3\right)-GA_{23}\left(U_z'+\omega_2-\frac{1}{R}U_x\right)\\
&+\frac{1}{R}GA_r\left(\omega_1'+f+\frac{1}{R}\omega_3\right)-GA_{2r}\left(\omega_1'+f-\frac{1}{R}U_y'+\frac{2}{R}\omega_3\right)\\
&+\frac{1}{R}GA_{3r}\left(U_z'+\omega_2-\frac{1}{R}U_x\right)=0
\end{aligned}\tag{A.1f}$$

$$\begin{aligned}
&-E\hat{I}_\phi f''-E\hat{I}_{\phi 2}\left(\omega_2''-\frac{1}{R}U_x''-\frac{1}{R^2}U_z'\right)\\
&+E\hat{I}_{\phi 3}\left(\omega_3''-\frac{1}{R}\omega_1'\right)+GA_r\left(\omega_1'+f+\frac{1}{R}\omega_3\right)\\
&+GA_{2r}\left(U_y'-\omega_3\right)+GA_{3r}\left(U_z'+\omega_2-\frac{1}{R}U_x\right)=0
\end{aligned}\tag{A.1g}$$

ii) Force-deformation relations of curved beam

$$\begin{aligned}
F_1&=EA\left(U_x'+\frac{1}{R}U_z\right)-\frac{1}{R}E\hat{I}_2\left(\omega_2'-\frac{1}{R}U_x'-\frac{1}{R^2}U_z\right)\\
&-\frac{1}{R}E\hat{I}_{\phi 2}f'+\frac{1}{R}E\hat{I}_{23}\left(\omega_3'-\frac{1}{R}\omega_1\right)
\end{aligned}\tag{A.2a}$$

$$\begin{aligned}
F_2&=GA_2\left(U_y'-\omega_3\right)+GA_{23}\left(U_z'+\omega_2-\frac{1}{R}U_x\right)\\
&+GA_{2r}\left(\omega_1'+f+\frac{1}{R}\omega_3\right)+g_y\left(U_y'-h_z\omega_1'\right)
\end{aligned}\tag{A.2b}$$

$$\begin{aligned}
F_3&=GA_3\left(U_z'+\omega_2-\frac{1}{R}U_x\right)+GA_{23}\left(U_y'-\omega_3\right)\\
&+GA_{3r}\left(\omega_1'+f+\frac{1}{R}\omega_3\right)+g_z\left(U_z'+h_y\omega_1'\right)
\end{aligned}\tag{A.2c}$$

$$\begin{aligned}
M_1&=GJ\left(\omega_1'+\frac{1}{R}\omega_3\right)+GA_r\left(\omega_1'+f+\frac{1}{R}\omega_3\right)\\
&+GA_{2r}\left(U_y'-\omega_3\right)+GA_{3r}\left(U_z'+\omega_2-\frac{1}{R}U_x\right)\\
&-g_yh_zU_y'+g_zh_yU_z'-\left(g_yh_z^2+g_zh_y^2\right)\omega_1'
\end{aligned}\tag{A.2d}$$

$$M_2 = E\hat{I}_2\left(\omega_2' - \frac{1}{R}U_x' - \frac{1}{R^2}U_z\right) + E\hat{I}_{\phi 2}f' - E\hat{I}_{23}\left(\omega_3' - \frac{1}{R}\omega_1\right) \quad \text{(A.2e)}$$

$$M_3 = E\hat{I}_3\left(\omega_3' - \frac{1}{R}\omega_1\right) - E\hat{I}_{\phi 3}f' - E\hat{I}_{23}\left(\omega_2' - \frac{1}{R}U_x' - \frac{1}{R^2}U_z\right) \quad \text{(A.2f)}$$

$$M_\phi = E\hat{I}_\phi f' + E\hat{I}_{\phi 2}\left(\omega_2' - \frac{1}{R}U_x' - \frac{1}{R^2}U_z\right) - E\hat{I}_{\phi 3}\left(\omega_3' - \frac{1}{R}\omega_1\right) \quad \text{(A.2g)}$$

Nam-Il Kim received his B.S. degree in Civil and Environmental Engineering from Sungkyunkwan University, Korea, in 1996. He then received his M.S. and Ph.D. degrees from Sungkyunkwan University in 1998 and 2004, respectively. Dr. Kim is currently a research professor at Civil and Environmental Engineering at Myongji University in Korea. Dr. Kim's research interests include stability and vibration of steel and composite structures.

Dong Ku Shin received his B.S. and M.S. degrees in Civil Engineering from Seoul National University, Korea, in 1983 and 1985, respectively. He then received his Ph.D. degree from Virginia Tech. at Blacksburg, VA, USA, in 1990. Dr. Shin is currently a professor of Civil and Environmental Engineering Department at Myongji University in Korea. Prof. Shin's research interests include LRFD design of steel bridges and stability of composite structures.